AD_____

AWARD NUMBER: W81XWH-04-1-0594

TITLE: Pre-clinical and Clinical Evaluation of High Resolution, Mobile Gamma Camera and Positron Imaging Devices

PRINCIPAL INVESTIGATOR: David R. Gilland, Ph.D.

CONTRACTING ORGANIZATION: University of Florida
Gainesville, FL 32611

REPORT DATE: October 2009

TYPE OF REPORT: Annual

PREPARED FOR: U.S. Army Medical Research and Materiel Command
Fort Detrick, Maryland 21702-5012

REPORT DOCUMENTATION PAGE

Form Approved
OMB No. 0704-0188

1. REPORT DATE	**2. REPORT TYPE**	**3. DATES COVERED**
1 October 2009	Annual	13 May 2008 – 20 Sep 2009

4. TITLE AND SUBTITLE

Pre-clinical and Clinical Evaluation of High Resolution, Mobile Gamma Camera and Positron Imaging Devices

5a. CONTRACT NUMBER

5b. GRANT NUMBER
W81XWH-04-1-0594

5c. PROGRAM ELEMENT NUMBER

6. AUTHOR(S)

David R. Gilland, Ph.D.

E-Mail: gilland@ufl.edu

5d. PROJECT NUMBER

5e. TASK NUMBER

5f. WORK UNIT NUMBER

7. PERFORMING ORGANIZATION NAME(S) AND ADDRESS(ES)

University of Florida
Gainesville, FL 32611

8. PERFORMING ORGANIZATION REPORT NUMBER

9. SPONSORING / MONITORING AGENCY NAME(S) AND ADDRESS(ES)
U.S. Army Medical Research and Materiel Command
Fort Detrick, Maryland 21702-5012

10. SPONSOR/MONITOR'S ACRONYM(S)

11. SPONSOR/MONITOR'S REPORT NUMBER(S)

12. DISTRIBUTION / AVAILABILITY STATEMENT
Approved for Public Release; Distribution Unlimited

13. SUPPLEMENTARY NOTES

14. ABSTRACT

The overall objective of this project is to design, build and evaluate a compact and mobile gamma and positron imaging camera. This imaging device has several advantages over conventional systems: (1) greater flexibility in positioning with respect to the target organ for improved spatial resolution and sensitivity, (2) the ability to image patients who cannot be transported to a radiology suite, (3) the potential for improved cost effectiveness for organ-specific imaging tasks compared with larger, general purpose imaging systems. Over the past year, the following tasks have been completed: (1) obtained human subjects research approval by University of Florida Institutional Review Board and U.S. Army Medical Research and Materiel Command (USAMRMC), Office of Research Protections (ORP), Human Research Protection Office (HRPO), (2) completed study on imaging performance using a cardiac thorax phantom including simulated perfusion defects, (3) advanced the development of a pinhole collimator for the mobile imaging system including final design specifications, fabrication of the collimator, and initial experimental performance evaluation.

15. SUBJECT TERMS
PET, SPECT, cardiac imaging, detectors

16. SECURITY CLASSIFICATION OF:			**17. LIMITATION OF ABSTRACT**	**18. NUMBER OF PAGES**	**19a. NAME OF RESPONSIBLE PERSON**
a. REPORT	**b. ABSTRACT**	**c. THIS PAGE**			**19b. TELEPHONE NUMBER** *(include area code)*
U	U	U	UU	20	USAMRMC

Table of Contents

INTRODUCTION

The overall objective of this project is to design, build and evaluate a compact and mobile camera for gamma and positron imaging. The purpose of this research is to produce an imaging device that has capabilities not currently found in other devices, that is, a device that can do bedside, tomographic nuclear medicine imaging. Over this past year, we have completed the human subjects approval process with both the University of Florida and the U.S. Army in order to begin the clinical evaluation of the device. We have performed extensive evaluations of the device using anthropomorphic cardiac phantoms that contain simulated perfusion defects. Finally, we have built a new collimator for the system using a pinhole geometry that has the potential for improved imaging characteristics compared with the conventional parallel hole collimator. This work is described in greater detail in the following section.

BODY

A request was made for a no-cost extension to this project due to the unforeseen delays that we have experienced in receiving the assembled detector from Jefferson Lab, which was reported in our last quarterly report. The request was made for a one year extension period. On November 10, 2009, we received the approval of this no-cost extension from the U.S. Army.

On October 28, 2009, the assembled detector was delivered to UF from Jefferson Lab. This detector is now undergoing basic performance evaluation. The detector will be evaluated with phantom objects before proceeding with the patient studies. We anticipate that the phantom studies should take approximately 2 months and the patient studies should take approximately 4 months.

Tasks 1 and 2 described below refer to the approved Statement of Work from the research proposal. This Statement of Work has been included in this report as Appendix 1.

Task 1: Perform clinical evaluation of cardiac PET imaging capability with patient images

On April 2, 2009 we received approval from the University of Florida Health Science Center Institutional Review Board for the clinical evaluation of the mobile imaging device. This approval, along with additional documentation, was then submitted to the U.S. Army for approval. On July 12, 2009 we received approval from U.S. Army Medical Research and Materiel Command (USAMRMC), Office of Research Protections (ORP), Human Research Protection Office (HRPO). The protocol was found to comply with applicable DOD, U.S. Army, and USAMRMC human subjects protection requirements.

The clinical evaluation will proceed immediately following the performance evaluation of the newly received detector. The detector will undergo the same evaluation as performed on the other detector (reported below) including the basic performance measurements using point sources and reconstructed image quality using the anthropomorphic cardiac phantom.

Task 2: Develop the cardiac SPECT imaging capability of the device and evaluate with experimental phantom data

Over the past year, we have performed extensive evaluations of the mobile imaging device for cardiac SPECT imaging. This work has culminated in a recently accepted manuscript for publication in the IEEE Transactions on Nuclear Science (publication #6 in “Reportable Outcomes” section and Appendix 2 in this annual report). Additional investigation has been undertaken to determine the ability of the mobile imaging device to image simulated perfusion defects in the anthropomorphic phantom. The defects are intended to mimic the characteristics

of perfusion defects in patient images for patients with coronary artery disease. This work was recently presented at the IEEE Nuclear Science Symposium and Medical Imaging Conference in Orlando, FL, on October 25-31, 2009. The poster that was presented at this conference is included as Appendix 3 in this report.

Figure 1 shows photographs of the cardiac phantom in position to be imaged by the mobile system. Also shown is the simulated perfusion defect, which can be filled with a known concentration of radioactivity, and positioned within the cardiac insert of the phantom. The hash marks next to the defect indicate centimeters. The defect is approximately 5 cm x 2 cm and occupies 25% of the circumference of the short axis of the phantom myocardium. For the F-18 studies with this phantom, the defect did not contain any radioactivity (100% contrast). For the Tc-99m studies, the defect either did not contain radioactivity or contain radioactivity at a concentration that was 50% of the concentration of the surrounding "normal" myocardium (50% contrast).

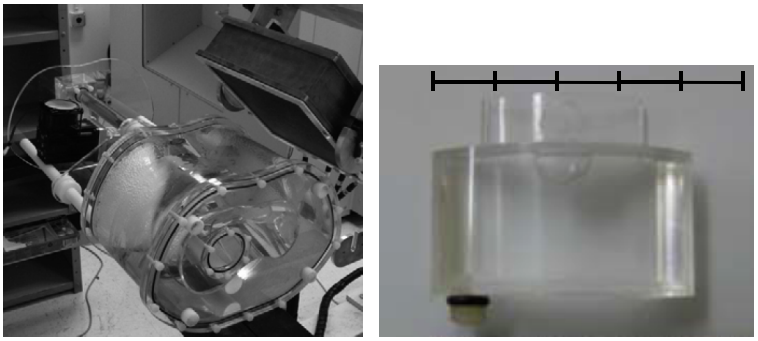

Fig. 1. Photograph showing anthropomorphic cardiac phantom (left) and simulated perfusion defect for cardiac insert.

The data acquisition in these phantom studies used 25 projection angles obtained over 180 degrees. There was out-of-field radioactivity placed in the liver compartment of the phantom. Long acquisition times were used, and a binomial thinning process was used to simulate lower acquisition times. The low acquisition times were effectively 15 minutes for the Tc-99m study and 20 minutes for the F-18 study with 200 μCi of activity in the myocardium and 400 μCi of activity in the liver compartment. A Metz filter was applied to the projection in order to reduce the effects of collimator septal penetration and to control noise. The detailed description of the Metz filter is given in publication #6 and Appendix 2. The projection data were reconstructed using the iterative MLEM method with 50 iterations.

The resulting images from the F-18 and Tc-99m studies are shown in Fig. 2. Each of the three rows of images in the figure represents a different slice through the short axis orientation. The left column in each of the two groupings shows the results without a perfusion defect present. Both low count statistics and high count statistics cases are presented. This figure verifies that the mobile imaging system is capable of detecting perfusion defects for both F-18 and Tc-99m for defects of this size and contrast.

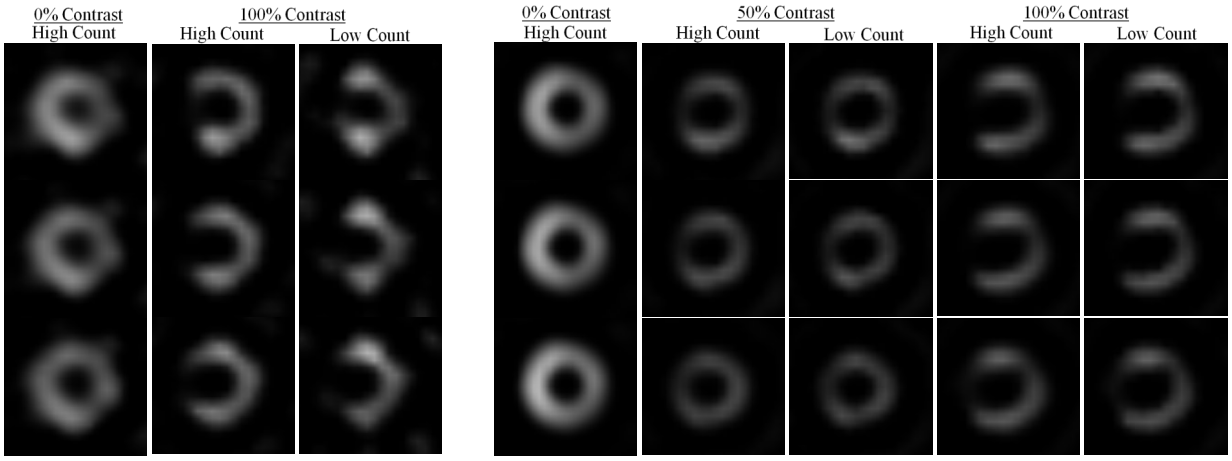

Fig. 2. Reconstructed short axis images of anthropomorphic cardiac phantom for F-18 (left) and Tc-99m (right) images.

The alternative approach that we have been investigating with this device is the use of a pinhole collimator. In the previous annual report we presented results of simulation studies that investigated this concept and guided the design of the collimator. Based on this design, over the past year we had a pinhole collimator built for this imaging system and have begun the initial testing of the collimator. Images were acquired of a point source and the cardiac phantom with a simulated perfusion defect using Tc-99m. An acquired projection image of the cardiac phantom with defect is shown in Fig. 3.

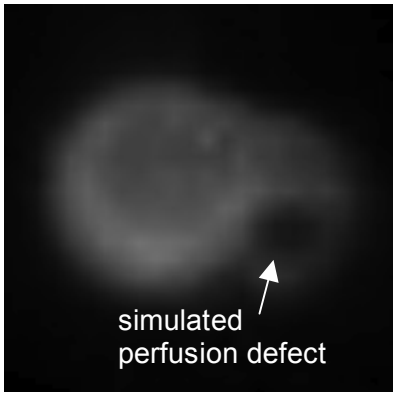

Fig. 3. Acquired projection image of cardiac phantom with defect using pinhole collimator

KEY RESEARCH ACCOMPLISHMENTS

- Obtained human subjects research approval by University of Florida Institutional Review Board and U.S. Army Medical Research and Materiel Command (USAMRMC), Office of Research Protections (ORP), Human Research Protection Office (HRPO) (Task 1)

- Completed study on imaging performance using a cardiac thorax phantom including simulated perfusion defects. This work has resulted in a recent peer-reviewed manuscript accepted for publication and a recent presentation at a scientific conference.

- Advanced the development of a pinhole collimator for the mobile imaging system including final design specifications, fabrication of the collimator, and initial experimental performance evaluation.

REPORTABLE OUTCOMES

Peer-reviewed publications directly supported by this grant

1. Tipnis U, Gilland DR, Smith MF, Drane WE, Majewski S. Design of a compact, mobile PET detector for bedside cardiac imaging. 2003 IEEE Nuclear Science Symposium Conference Record, 19-25 Oct, 2003, vol. 4, pp. 2438-2441.
2. Tipnis U, Smith MF, Turkington TG, Wilson J, Majewski S, Kross B, Wojcik R, Gilland DR. A simulation study of a bedside cardiac PET imager. 2004 IEEE Nuclear Science Symposium Conference Record, 16-22 Oct, 2004, vol. 5, pp. 3126-3129.
3. Studenski MT, Parker JG, Gilland DR, Majewski S, Hammond B. Performance evaluation of a small field-of-view, mobile PET/SPECT system. *2007 IEEE Nuclear Science Symposium Conference Record*, 26 Oct. – 3 Nov., vol. 5, pp. 3770-3, 2007.
4. Weisenberger AG, Majewski S, Gilland DR, Hammond W, Kross B, Popov V, Proffitt J, Mckisson J, Smith MF, Zorn C. Implementation of a mobile cardiac PET imager for the emergency room and intensive care unit. *2007 IEEE Nuclear Science Symposium Conference Record*, 26 Oct. – 3 Nov., vol. 5, pp. 3705-8, 2007.
5. Studenski MT, Gilland DR, Parker JG, Majewski S, Hammond W, Weisenberger A, Popov V. Performance evaluation of a bedside cardiac SPECT system, *Transactions on Nuclear Science*,56:625-632, 2009.
6. Studenski MT, Gilland DR. Acquisition and processing methods for a bedside cardiac SPECT imaging system. *Transactions on Nuclear Science*, accepted for publication, October, 2008.
7. Studenski MT, Gilland DR. Design and simulation of a pinhole collimator for 511 keV mobile SPECT imaging. November, 2009, in preparation.

Abstracts and presentations at scientific meetings directly supported by this grant

1. Dingley J, Tipnis UJ, Gilland DR. Cardiac 511 keV SPECT simulation with a compact detector design. Presented at: 2005 Nuclear Science Symposium and Medical Imaging Conference, October 23-29, Fajardo, Puerto Rico.
2. Majewski S, Gunning W, Hammond W, Kross B, Smith M, Popov V, Proffitt J, Weisenberger A, Wojcik R, and Gilland D. Development and Evaluation of Detector Heads and Readout for a Mobile Cardiac Imager System, Presented at: 2006 IEEE Nuclear Science Symposium and Medical Imaging Conference, Oct. 29 – Nov. 3, San Diego, CA.
3. Weisenberger AG, Majewski S, Gilland DR, Hammond W, Kross B, Popov V, Proffitt J, Mckisson J, Smith MF, Zorn C. Implementation of a mobile cardiac PET imager for the emergency room and intensive care unit. Presented at: 2007 IEEE Nuclear Science Symposium and Medical Imaging Conference, Oct. 27 – Nov. 3, Honolulu, HI.

4. Studenski MT, Parker JG, Gilland DR, Majewski S, Hammond B. Performance evaluation of a small field-of-view, mobile PET/SPECT system. Presented at: 2007 IEEE Nuclear Science Symposium and Medical Imaging Conference, Oct. 27 – Nov. 3, Honolulu, HI.
5. Studenski MT, Gilland DR, Parker JG. A Small Field-of-View, Mobile PET/SPECT System for Bedside Environments: A Dynamic Cardiac Phantom Study using 99mTc and 18F-FDG. Presented at the American Association of Physicists in Medicine 50th Annual Meeting, July 27-31, 2008, Houston, TX.
6. Studenski MT, Gilland DR. Acquisition and Processing Methods for a Bedside Cardiac SPECT Imaging System. Presented at the IEEE 2008 Nuclear Science Symposium and Medical Imaging Conference, October 18-25, 2008, Dresden, Germany.
7. Cebula A, Studenski MT, Samarin A, Gilland DR, Evaluation of a Bedside SPECT Imaging System based on Myocardial Defect Detection. Presented at the 2009 IEEE Nuclear Science Symposium and Medical Imaging Conference, Oct. 25-31, 2009. Orlando, FL.

Degrees awarded that were directly supported by this grant

1. Matthew Studenski, Masters of Science, Department of Nuclear and Radiological Engineering, University of Florida, May 2008.
2. Matthew Studenski, Doctor of Philosophy, Department of Nuclear and Radiological Engineering, University of Florida, May 2009.

CONCLUSIONS

During the past year, we have made progress in the following areas: we have completed the human subjects approval process with both the University of Florida and the U.S. Army in order to begin the clinical evaluation of the device, we have performed extensive evaluations of the device using anthropomorphic cardiac phantoms that contain simulated perfusion defects, and we have built a new collimator for the system using a pinhole geometry that has the potential for improved imaging characteristics compared with the conventional parallel hole collimator.

The medical benefits that can result from this device can be potentially substantial, not only for the military health care system but also for health care of the general population. This device will be capable of delivering critical diagnostic imaging (PET and SPECT) to patients who otherwise cannot benefit from these technologies. Also, this device potentially can be a cost effective alternative to conventional PET systems for cardiac imaging. Finally, with the accelerated growth in the development of imaging agents for PET and SPECT, there will be a greater need for novel and dedicated imaging devices, such as the device developed in this project.

APPENDICES

The following appendices are included as attachments to this report:

1. Project Statement of Work
2. Draft of: Studenski MT, Gilland DR, Cebula AT. Acquisition and processing methods for a bedside cardiac SPECT imaging system. *Transactions on Nuclear Science*, accepted for publication, October, 2009.

3. Cebula AT, Studenski MT, Samarin A, Gilland DR. Evaluation of a bedside SPECT system based on cardiac phantom defect detection. Presented at the 2009 IEEE Nuclear Science Symposium and Medical Imaging Conference, October 25-31, 2009, Orlando, FL.

Statement of Work

Pre-clinical and Clinical Evaluation of High Resolution, Mobile Gamma Camera and Positron Imaging Devices
FY 2007

Technical Objectives 1 and 2 were included in the original proposal as Optional (unfunded) years 1 and 2.

1. Perform clinical evaluation of cardiac PET imaging capability with patient images
    a. Develop imaging software
        i. Data transfer protocol from camera computer to image processing workstation
        ii. Image reconstruction and manipulation tools
        iii. Image display format
    b. Clinical evaluation: Phase I. Patients 1-4. Optimize:
        i. Injected activity level based on detector count rate capability
        ii. Detector positioning (detector-to-detector, detector-to-patient)
        iii. Background (randoms, scatter) subtraction method
        iv. Image reconstruction methods
    c. Clinical evaluation: Phase II. Patients 5-20
        i. Apply optimized image processing
        ii. Clinical assessment: diagnostic quality scoring

2. Develop the cardiac SPECT imaging capability of the device and evaluate with experimental phantom data
    a. Collimator design and simulation studies for high energy imaging
        i. Parallel hole and pinhole collimator design tools
        ii. Develop simulation software: analytical, Monte Carlo
    b. Image reconstruction algorithm development
        i. Analytical vs. iterative methods
        ii. Corrections for scatter, collimator penetration
        iii. Evaluate effects of number of angles, angular range, and dwell time based on reconstructed spatial resolution, heart phantom image quality
    c. Collimator fabrication
    d. Performance evaluation with experimental phantoms
        i. Spatial resolution (planar and SPECT, line source and cold rod phantoms)
        ii. Sensitivity in air and water
        iii. Cardiac SPECT phantom image quality

Acquisition and Processing Methods for a Bedside Cardiac SPECT Imaging System

Matthew T. Studenski, *Student Member, IEEE*, David R. Gilland, *Member, IEEE,* and Alan Cebula, *Student Member, IEEE*

Abstract— We have developed a compact and mobile gamma imaging system that is designed for both PET and SPECT acquisitions within a bedside environment, such as an intensive care unit, surgical suite, or emergency room. This paper describes the SPECT performance evaluation of the system for cardiac imaging, including both Tc-99m and F-18 radionuclides. For cardiac F-18 imaging in a bedside environment, the 511 keV SPECT approach using high energy collimation and anterior 180 degree acquisition has the advantages of not requiring a detector to be positioned beneath the bed and greatly reducing attenuation effects. In this study, we evaluated SPECT reconstructed image quality using an anthropomorphic dynamic cardiac phantom filled with Tc-99m and F-18 separately. The specific issues that were addressed in this study included the following: 1) mitigating septal penetration effects with the 511 keV photons using de-convolution filtering, 2) reducing truncation effects due to the relatively small field-of-view of the camera using angle-dependent center-of-rotation shifts, and 3) investigating the effects of reduced angular sampling and angular range. We found that reducing angular sampling to 28 projections through 135 degrees with Tc-99m and 25 projections through 180 degrees with F-18 showed all features of the myocardium.

***Index Terms*—Cardiac imaging, image processing, mobile PET, mobile SPECT**

I. Introduction

We have developed a compact and mobile gamma imaging system that is designed for both PET and SPECT acquisitions within a bedside environment, such as an intensive care unit, surgical suite, or emergency room. The system consists of two compact detectors (25 cm × 25 cm active area) containing pixilated NaI scintillators (5 mm × 5 mm, 12.5 mm thick) and position-sensitive photomultiplier tubes. The detectors are mounted to a mobile gantry[1] that allows flexible detector motion and positioning for tomographic PET and SPECT imaging (Fig. 1). Details of the detector and gantry design and operation have been previously described in [1] and [2].

Fig. 1. Mobile gantry with detectors in an oblique and lateral orientation for SPECT imaging along with the associated mobile electronics rack seen to the right.

One of the key applications for this system is cardiac emission tomography, including both myocardial perfusion imaging using Tc-99m tracers and viability imaging using F-18 tracers [3]-[7]. For cardiac F-18 imaging in a bedside environment, the 511 keV SPECT approach using high energy collimation and an anterior 180 degree acquisition has the advantages of not requiring a detector to be positioned beneath the bed and greatly reducing attenuation effects.

The basic system performance measurements in planar and SPECT modes using both Tc-99m and F-18 point sources were described previously [2]. The low energy collimator for Tc-99m has 23 mm hole length, 1.5 mm hole diameter, and 0.2 mm septal thickness. The high energy collimator for F-18 has 49 mm hole length, 2.3 mm hole diameter, and 2.02 mm septal thickness. We found the spatial resolution at 10 and 20 cm to be 1.14 and 1.64 cm FWHM at 140 keV and 1.52 and 2.04 cm FWHM at 511 keV. The reconstructed SPECT spatial resolution near the center-of-rotation with a radius-of-rotation

Manuscript received October 30, 2008. Revision submitted October 14, 2009. This work was supported in part by the U.S. Army Medical Research and Material Command under award No. W81XWH-04-1-0954.

Matthew T. Studenski is with the Department of Nuclear and Radiological Engineering Department at the University of Florida, Gainesville, FL 32611 USA (telephone: 352-846-3066; e-mail: mstudens@ ufl.edu).

David R. Gilland is with the Nuclear and Radiological Engineering and Biomedical Engineering Departments at the University of Florida, Gainesville, FL 32611 USA. (e-mail: gilland@ufl.edu).

Alan Cebula is with the Department of Nuclear and Radiological Engineering at the University of Florida, Gainesville, FL 32611 USA (e-mail: acebula@ufl.edu).

[1] Manufactured by Advanced Development Solutions, Phillipsburg, NJ, 08865

Fig. 2. The dynamic cardiac phantom and the bedside imaging system with the detector head in a left oblique position (45 degrees).

of 20 cm was measured to be 1.59 cm with Tc-99m and 1.58 cm with F-18 and the sensitivity was measured to be 4.15 counts/μCi/s with Tc-99m and 0.67 counts/μCi/s with F-18. Here, we further this system evaluation by considering reconstructed image quality using an anthropomorphic dynamic cardiac phantom[2] to simulate a more realistic source distribution and out-of-field activity (Fig. 2).

Three key factors for the imaging system are specifically addressed in this cardiac phantom study: 1) mitigating the effects of septal penetration photons for the 511 keV SPECT data, 2) reducing truncation effects due to the relatively small field-of-view (FOV) of the detector, and 3) investigating the effects of reduced angular sampling and angular range.

To compensate for septal penetration effects, this study uses a Metz de-convolution filter which incorporates the measured 2D modulation transfer function (MTF) including septal penetration effects. The underlying assumption is that the septal penetration effects in the measured data can be modeled as a linear, spatially-invariant process. This method of septal penetration compensation was investigated previously for In-111 and I-123 imaging by King, *et al*. [8].

Due to the relatively small FOV of the detectors, truncation of the myocardium can arise in the tomographic image, particularly in regions distant from the axis-of-rotation. In order to overcome this problem in this study, at each projection angle during the acquisition, the detector is translated tangentially to maintain the heart near the center of the FOV. This is effectively an angle-dependent center-of-rotation (COR) shift that is recorded and modeled in the reconstruction. Although this prevents truncation of the myocardium, there will likely be truncation of surrounding tissues, which is unavoidable with this small field-of-view system.

In this study we investigate the effects of angular sampling and angular sampling range on the resulting reconstructed image. Theoretically, it has been noted that the required number of angular samples changes linearly with the linear sampling distance and inversely with the field-of-view (FOV) size [9]. Comparing the FOV of this system (25 cm) to that of a traditional system (typically 50 cm), the required number of angular samples with this system is reduced by a factor of two relative to a traditional SPECT system. We would like to determine the minimum number of angular samples required since detector positioning with this prototype system is done manually, meaning that the detector is rotated to the desired angle, and then is moved horizontally and vertically until it is as close to the phantom as possible to maximize the spatial resolution at each projection angle. Subsequent system designs could have automated positioning but it is not clear that for a mobile SPECT system, automated angle stepping, like conventional SPECT systems, will be the method of choice. In order to achieve a minimum source-to-detector distance for best spatial resolution at all angles, and an economical design, it is possible that manual positioning will be preferred. Clearly, the manual approach requires greater operator effort. In the manual positioning case, determining the minimum required number of angles is important.

Previous work on limited angular range (i.e. less than 360 degrees) has been used to reduce the overall acquisition time and improve image contrast [10], [11]. Our investigation of the reduced angular sampling range is motivated by our expectation that for applications such as ICU bedside imaging, it may be difficult to obtain quality lateral views of the patient if they are not capable of lifting their arms.

II. Methods

A. Experimental phantom

The dynamic cardiac phantom (Fig. 2) consists of a water filled torso, a beating heart composed of an inner and outer latex membrane, two lungs filled with one part water and two parts Styrofoam beads to simulate the density of the lungs, a Teflon spine, and a water filled liver. The volume contained between the two membranes of the beating heart can be filled with Tc-99m to simulate a myocardial perfusion study or with F-18 to simulate a myocardial viability study. A computer controlled pump is used to expand and contract the myocardium and values for stroke volume, ejection fraction, and beats per minute (BPM) can be input to the controlling computer. For this investigation, the phantom was programmed for 72 BPM, 45% ejection fraction, and 55 mL stroke volume.

For both the Tc-99m and F-18 studies, the phantom myocardium was filled with approximately 1 mCi of activity and the phantom liver (1700 mL) was filled with approximately 2 mCi of activity. For the F-18 studies, in order to isolate the effects of out-of-field activity, additional acquisitions were performed with no activity in the liver.

B. Data acquisition

Acquisitions consisted of 37 projection angles equally spaced over 180 degrees. The energy window was 20% centered on the photopeak. Relatively high count, low noise projection data were acquired for both the Tc-99m and F-18 studies, and a count thinning technique was used to generate lower count data from this high count data [12]. This

[2] Model ECT/DY-CAR/P, Data Spectrum Corp. Hillsborough, NC, 27278

technique involves replacing each pixel value in the high count data with a sample from a binomial distribution with number of trials *n* equal to the high count pixel value and probability of success *p* equal to the desired scale factor. This is a convenient way to scale down the count level while maintaining the Poisson statistics of the measured data. For the Tc-99m study, the high count data were obtained using an approximately 55 minute acquisition time, which resulted in 2.5×10^5 total counts per projection. The F-18 data were obtained using an approximately 80 minute acquisition time with approximately 3.0×10^5 total counts per projection. One change from the 37 projection angle protocol was that the F-18 acquisition containing out-of-field activity was done with 25 projection angles resulting in a 60 minute acquisition time.

In order to simulate the increased noise that results from shorter acquisition times, a count thinning technique was applied to the high count projection data. The count thinning approach was used to scale down the projection data by factors of 2, 4, and 8.

C. Metz filtering of the projection data

In planar images of an F-18 point source, low intensity "tails" due to septal penetration by the 511 keV photons are observed [2], [6]. In order to conserve weight, the high energy collimator was designed to allow a 7% penetration level rather than the conventional 5% [13]. To mitigate this septal penetration effect in this study, we filter the projection data prior to the reconstruction using a 2D Metz filter, which is a combination of a de-convolution and smoothing filter [14].

The Metz filter function is given in (1) where MTF(υ) is the 2D modulation transfer function and parameter X determines the extent to which the filter follows the inverse MTF before rolling off to zero gain. We tested a range of values for X (50, 100, and 200) for the F-18 filter and negative values in the filtered images were set to zero.

$$\mathrm{Metz}(\tilde{\upsilon}) = \frac{1-\left(1-\mathrm{MTF}(\tilde{\upsilon})^2\right)^X}{\mathrm{MTF}(\tilde{\upsilon})} \qquad (1)$$

The 2D MTF for the Metz filter was obtained from measured point spread functions using an F-18 point source (5 mm in diameter and 20 cm from collimator) and is shown in Fig. 3 along with the point spread function from a similar Tc-99m point source. The star pattern due to collimator septal penetration is evident and is not seen in the 140 keV point source image. We acknowledge that the MTF is distance dependent and we chose 20 cm as an average source-to-detector distance over all the projections covering 180 degrees. We also tested the Metz filter on the Tc-99m data to study its effect on the final reconstructed image. For the Tc-99m projections, we tested the filter with values of 2, 5, and 10 for X in (1).

The first step in processing the projection data was to obtain the MTFs for both Tc-99m and F-18. Fig. 4 shows the MTFs along with horizontal and vertical profiles. From the calculated MTFs, the 2D Metz filter was created. Fig. 5 shows horizontal and vertical profiles from the 2D Metz filters with different values of X tested for the Tc-99m and F-18 acquisitions.

D. Image reconstruction

Because of the small field-of-view of this system, the conventional method of orbiting the detector about a fixed axis located near the body axis can result in truncation of the heart region, as shown in Fig. 6A. In order to eliminate the truncation of the myocardium, at each projection angle the detector is shifted tangentially to maintain the myocardium near the center of the FOV (Fig. 6B). This angle-dependent shift (effectively an angle-dependent "center-of-rotation" shift) is accounted for within the reconstruction algorithm.

For each projection, the horizontal and vertical position of the detector, and the detector angle are recorded. The angle-dependent shift is computed using simple trigonometric equations. The MLEM reconstruction algorithm (50 iterations for Tc-99m and 200 iterations for F-18) was used to reconstruct the images without attenuation, scatter, or detector response corrections applied [15]. These iteration stopping points, combined with the Metz filter, were chosen subjectively. The reconstruction times were approximately 10 seconds for the Tc-99m images and 40 seconds for the F-18 images.

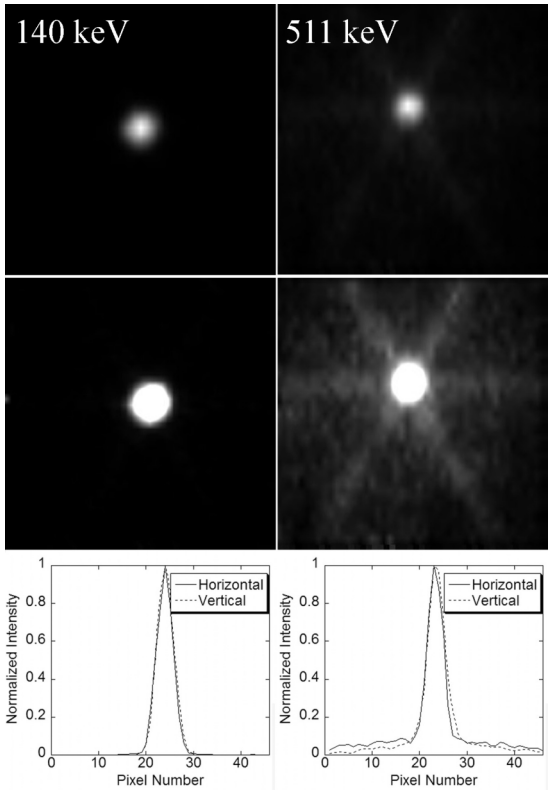

Fig. 3. Point source images for 140 keV and 511 keV sources without windowing (top), windowed to 33% of the maximum pixel intensity (middle), and the corresponding horizontal and vertical profiles (bottom). The FOV in both images is 25×25 cm^2.

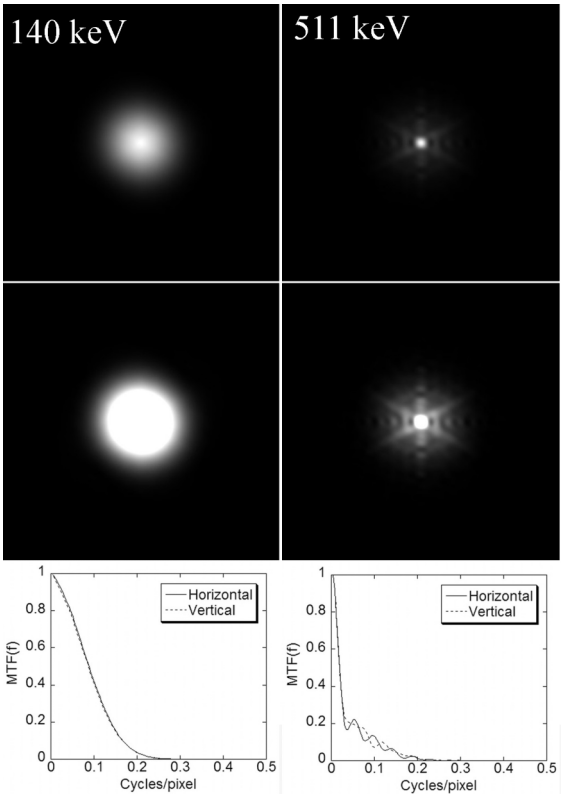

Fig. 4. MTF (top) and MTF windowed to 33% of the maximum pixel intensity (middle) with the corresponding horizontal and vertical profiles (bottom) for both 140 and 511 keV point sources used in calculating the Metz filter.

E. Effect of angular sampling

One of the goals of this paper was to investigate the effect of reduced angular sampling and angular range on reconstructed image quality. To test how limiting the number of projection angles affected the final reconstructed images, we reduced the number of projections reconstructed from 37 to 19 and 10 evenly spaced projection angles through 180 degrees. The count level was adjusted for the three cases by count thinning to simulate a constant acquisition time. To test the effect of reduced angular sampling range, the anterior 135 and 90 degrees of projection data were extracted and reconstructed. A constant acquisition time was simulated for these tests as well.

F. Comparison with a commercial SPECT system

To compare the performance of the mobile system to a traditional SPECT system with Tc-99m, we acquired data of the dynamic cardiac phantom on a commercial SPECT system[3] with low energy, ultra-high resolution collimators. The phantom myocardium was filled with Tc-99m and a 180 degree, 64 projection acquisition was obtained at a moderately high count level (approximately 2.15×10^5 counts within a mid-ventricular 3 mm transaxial slice resulting in an acquisition time of approximately 20 minutes). The projections were obtained over the anterior 180 degrees, as with the mobile system. No activity was added to the phantom liver and no attenuation, scatter, or detector response corrections were applied to the MLEM reconstruction (50 iterations). We compared this data to a 15 minute, 37 projection acquisition with Tc-99m and out-of-field activity obtained with the mobile system.

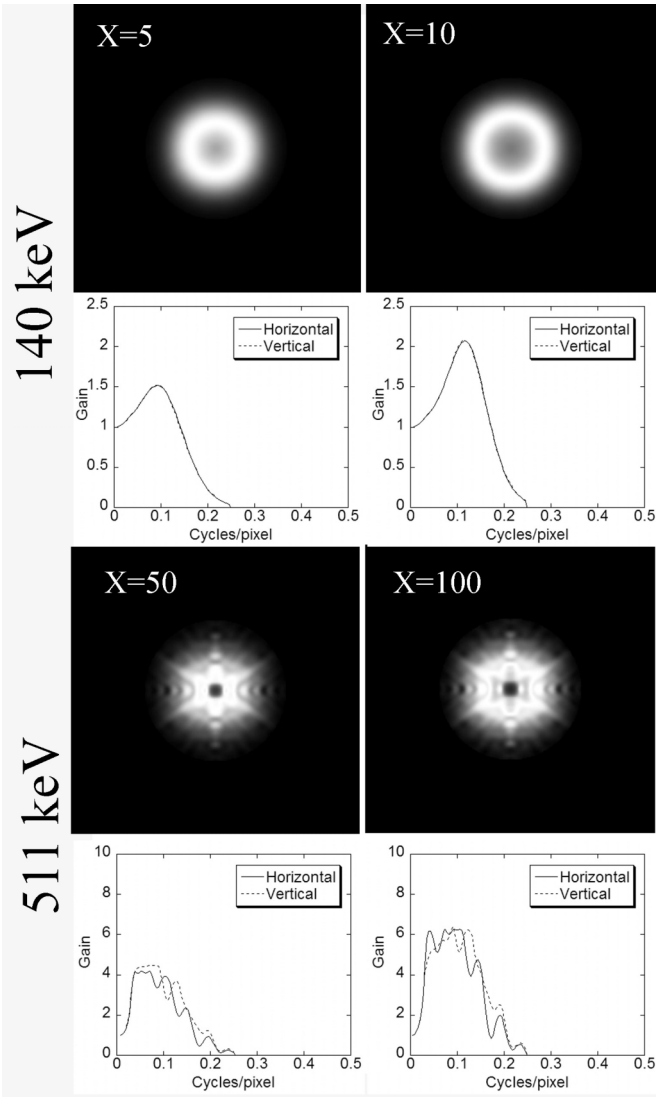

Fig. 5. Metz filters and the associated horizontal and vertical profiles for both 140 keV and 511 keV with different values for X.

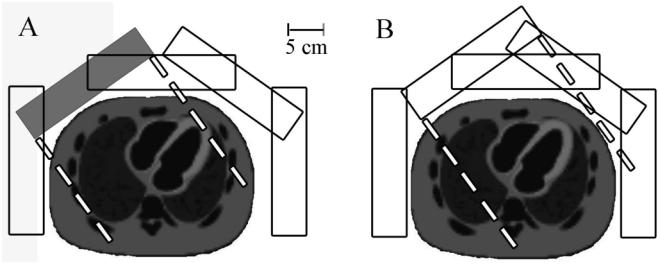

Fig. 6. Five projection angles demonstrating how myocardial truncation results in the fixed axis acquisition protocol (A) while the new protocol (B) eliminates truncation of the myocardium (but not surrounding tissue). The shaded detector's position causes myocardial truncation as shown by the dashed lines indicating the edges of the FOV.

[3] Triad 88, Trionix Research Laboratory, Twinsburg, OH 44087

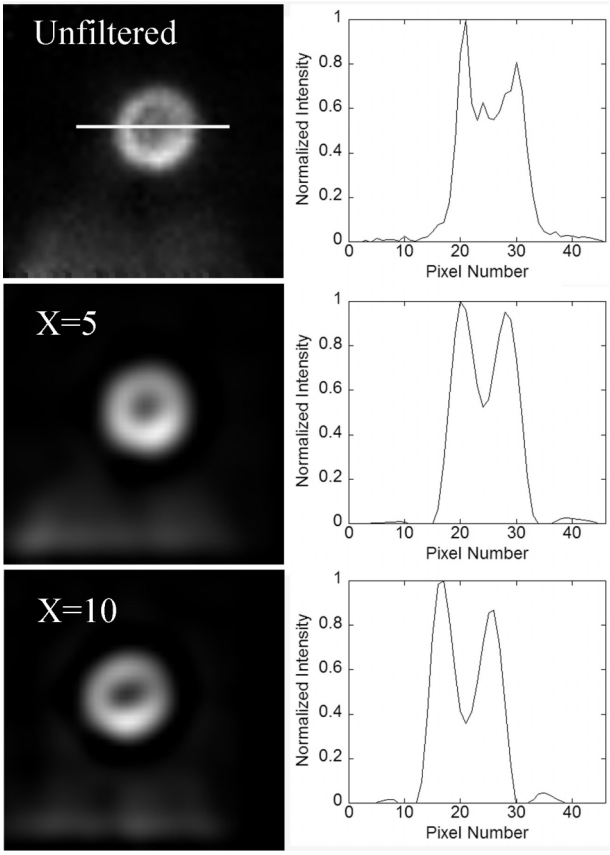

Fig. 7. Projection images obtained at 45 degrees using Tc-99m and out-of-field activity with varying degrees of filtering.

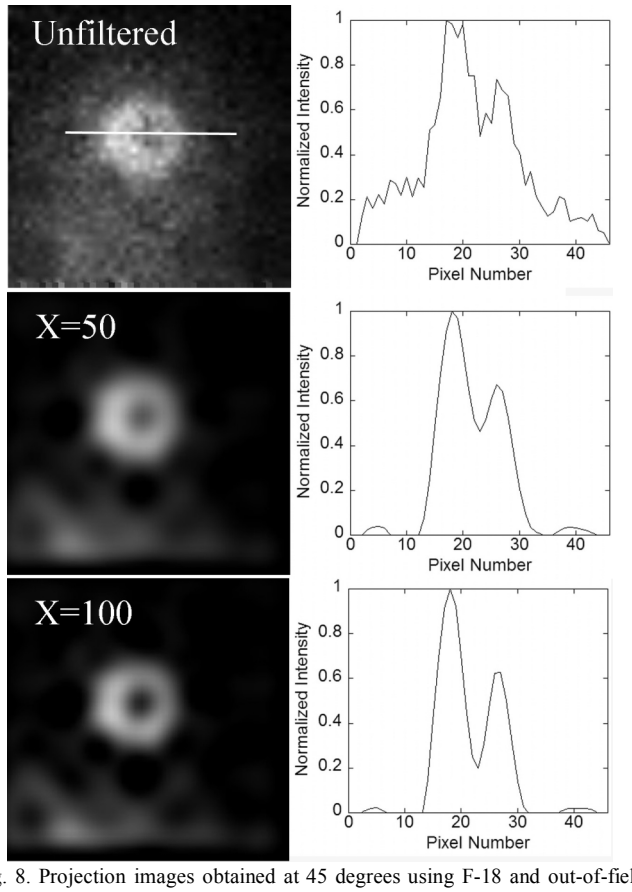

Fig. 8. Projection images obtained at 45 degrees using F-18 and out-of-field activity with varying degrees of filtering.

G. *Myocardial defect study*

As an initial test to assess reconstructed image quality with a myocardial defect present, we obtained a fillable plastic defect (4 cm wide by 2 cm tall by 1 cm thick) that was filled with water without activity. We inserted this defect in the myocardium of the dynamic cardiac phantom and acquired 25 projection angles with 300 kcts/projection over the anterior 180 degrees. Two acquisitions were performed (Tc-99m and F-18). Each was 40 min. with 1 mCi of activity in the myocardium and 2 mCi in the liver to simulate out-of-field activity.

These acquisitions provided high count, low noise images. From this high count data, lower count data were generated using binomial thinning of the measured projection data to reduce the count level by a factor of four.

Projection data were reconstructed using 50 iterations of MLEM. The reconstructed images were reoriented into short axis slices. Profiles of the short axis slices were obtained through the myocardial defect region.

III. RESULTS

A. *Septal penetration compensation*

Figs. 7 and 8 show 45 degree projection images from the Tc-99m and F-18 acquisitions (with out-of-field activity), respectively, with the varying degrees of filtering. Detected events outside of the myocardium are more pronounced in the F-18 images, as expected, due to septal penetration. The Poisson noise in this region is evident. Larger values of the Metz filter parameter were used with the F-18 data in order to effectively compensate for septal penetration effects in the F-18 data. The parameter value of 100 with the F-18 data, while

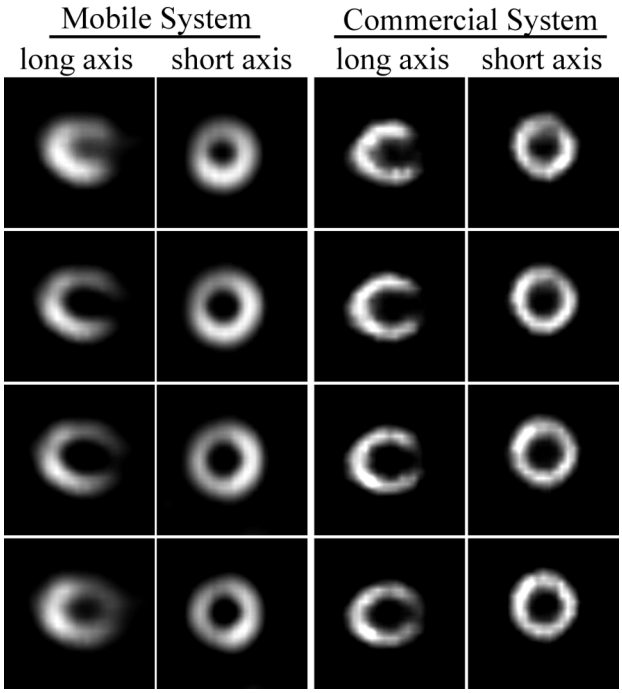

Fig. 9. Comparison of the mobile system's performance to a commercial system using the dynamic cardiac phantom and Tc-99m. The mobile system used 37 angles over 180 degrees and the commercial system used 64 angles over 180 degrees.

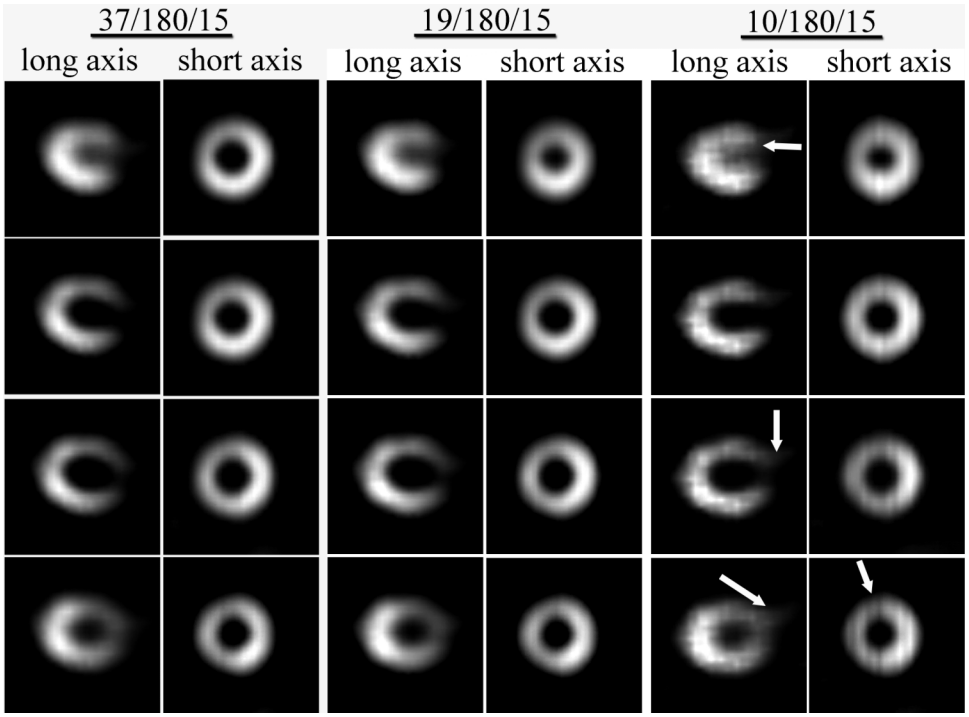

Fig. 10. Four long axis and four short axis slices from the 15 minute Tc-99m acquisitions with 37 (highest sampling), 19, and 10 projection angles. Artifacts in the images are indicated by the white arrows.

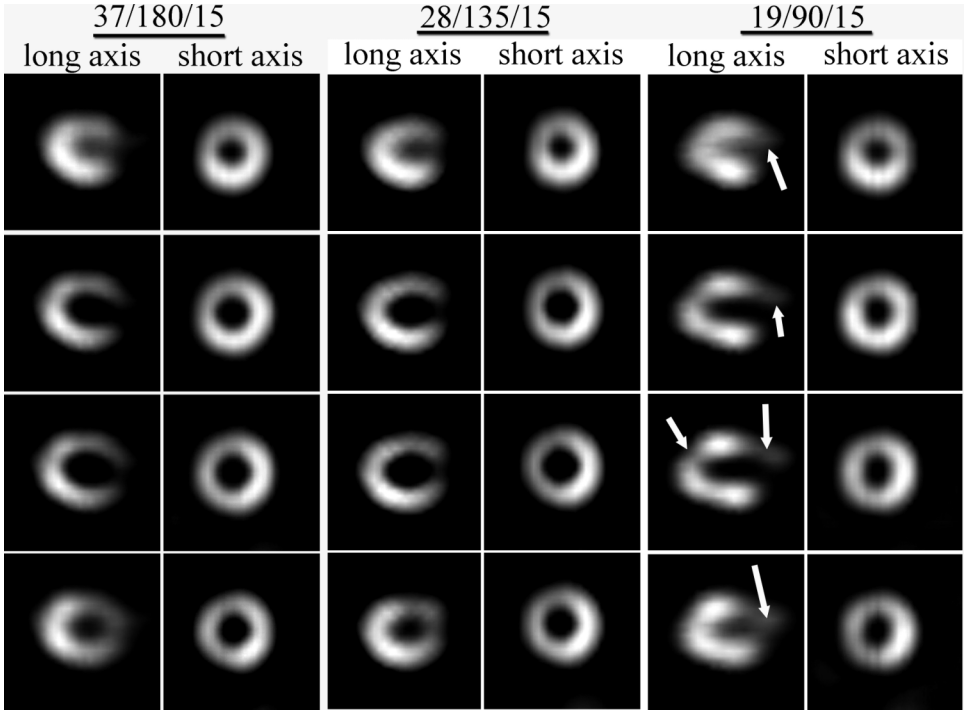

Fig. 11. Four long axis and four short axis slices from the Tc-99m 180 degree (highest sampling), 135 degree, and the 90 degree angular coverage acquisition. Artifacts are indicated by the white arrows.

greatly reducing penetration effects, produced large negative values in the projection data that require truncation before reconstruction. The remainder of the results focus on X=5 for Tc-99m and X=50 for F-18.

B. Comparison with a commercial SPECT system

Fig. 9 shows four long and short axis slices from both the commercial system acquisition and our 37 projection acquisition with the mobile system. The commercial system showed superior spatial resolution demonstrated by the thinner, more defined myocardium and superior statistical variation demonstrated by the even activity distribution throughout the myocardium. The differences in spatial resolution can be attributed to differences in collimator spatial resolution ("ultra-high" spatial resolution for the commercial system and general purpose class of spatial resolution with the

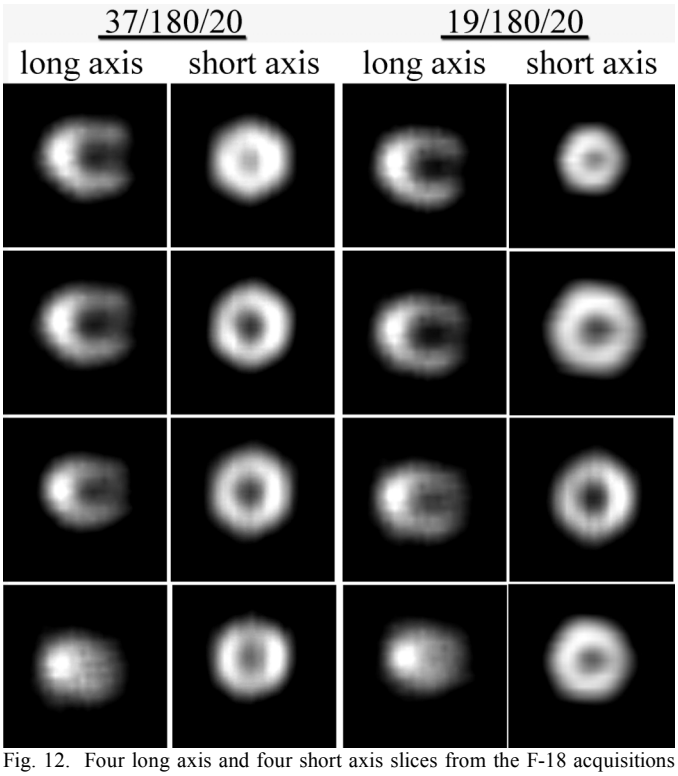

Fig. 12. Four long axis and four short axis slices from the F-18 acquisitions without activity in the liver and 37 and 19 projection angles.

mobile system) and also potentially to differences in angular sampling. The images with the commercial system provide a gold standard for image quality comparison, although bedside SPECT imaging is not possible with the commercial system.

C. *Effect of angular sampling*

1) *Tc-99m*

For the remainder of the paper, the figures are labeled in terms of number of projection angles / angular coverage in degrees / total acquisition time in minutes, as seen above the images in Fig. 10. Fig. 10 shows four slices in both the short and long axis planes from 15 minute acquisitions with 37 (highest sampling), 19, and 10 projection angles. This figure demonstrates that reducing the number of projection angles to 19 does not appreciably affect the image quality when using Tc-99m. Fig. 10 also shows that reducing the sampling in an extreme case to 10 projections degrades the images both with streaking artifacts outside the myocardium and dark streaks in the myocardium.

We also wanted to test the effect of reducing the angular coverage from 180 degrees. We observed that reducing the angular coverage to 135 degrees did not severely degrade reconstructed image quality (Fig. 11). Fig. 11 also showed that severely limited angular coverage (90 deg.) introduced substantial streak artifacts. In a clinical situation, reducing the angular coverage would only be recommended if the bedside environment prevented full 180 degree angular coverage.

2) *F-18*

Fig. 12 shows the reconstructed image slices from the F-18 data without out-of-field activity in the liver. Compared with the Tc-99m images with similar angular sampling, the F-18 images exhibit somewhat degraded spatial resolution of the myocardium walls and a reduced ventricle-to-myocardium contrast. This effect is due mainly to the propagation of the septal penetration patterns in the reconstruction. These effects become more pronounced in the 19 angle images although the overall shape of the myocardium is accurately depicted. The reduced angular sampling images also exhibited streaking artifacts that resulted from interpolation when the reconstruction was reoriented into long and short axis slices. These streaks are not seen in the projection images (Figs. 7 and 8) or in the original reconstruction.

Fig. 13 shows the F-18 results with liver activity present compared to the highly sampled acquisition without activity in the liver. Also included in the figure are unprocessed projection images with and without background activity. These images begin to show a distortion of the shape of the myocardium and a small level of intensity artifacts (hot and cold spots) that are not observed in the images without liver activity. The streaking artifacts from interpolation are also present as before.

As with the Tc-99m acquisitions we reconstructed images with reduced angular coverage, but reducing the angular coverage to less than 180 degrees resulted in more severe streaking artifacts.

D. *Myocardial defect study*

Fig. 14 shows the reconstructed short axis images and location of the profiles used for comparison. There is minimal difference between the high and low count images for Tc-99m. The low count F-18 image shows increased noise and artifacts compared to the high count F-18 image.

Comparing the F-18 images with the Tc-99m images, the effects of septal penetration with the high energy emitter can be seen. In the F-18 images, there is a greater level of extra-myocardial intensity including in the ventricle region. Fig. 15 shows the increase in image noise for lower count acquisitions. For F-18, the effect of image noise appears as hot and cold spots in the image.

IV. Summary and Discussion

This paper presents the SPECT performance evaluation of a mobile gamma imager for cardiac applications using Tc-99m and F-18. The system employed angle-dependent projection shifting to reduce truncation effects and de-convolution filtering to control septal penetration effects with F-18. We chose the Metz filter over a simple low pass filter in order to de-convolve the low frequency tails in the point spread function that result from septal penetration. Like a low-pass filter, the Metz filter is also capable of controlling high frequency noise by rolling off to zero gain at high frequency.

Another possible means of reducing the effect of septal penetration is to use the point response function in an iterative reconstruction algorithm [16]. This method has been shown to be effective although it requires greater computation than simple de-convolution filtering.

The results using a dynamic cardiac phantom showed that

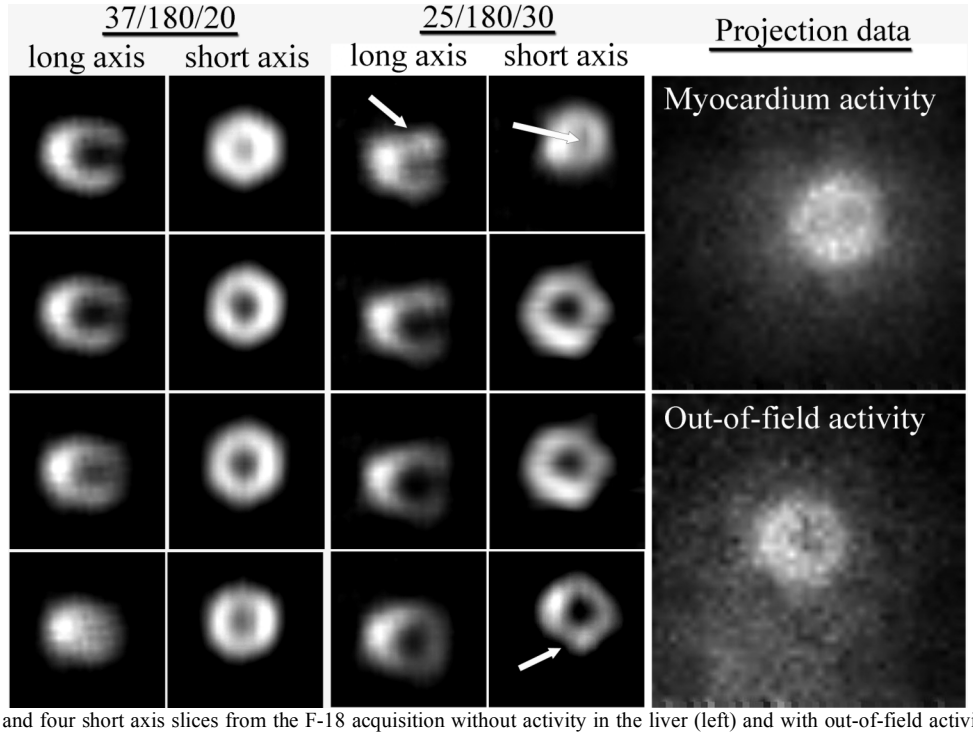

Fig. 13. Four long axis and four short axis slices from the F-18 acquisition without activity in the liver (left) and with out-of-field activity in the liver (middle). Artifacts are indicated by the white arrows. The projection data (unprocessed) to the right shows the effect of penetration photons from the out-of-field activity.

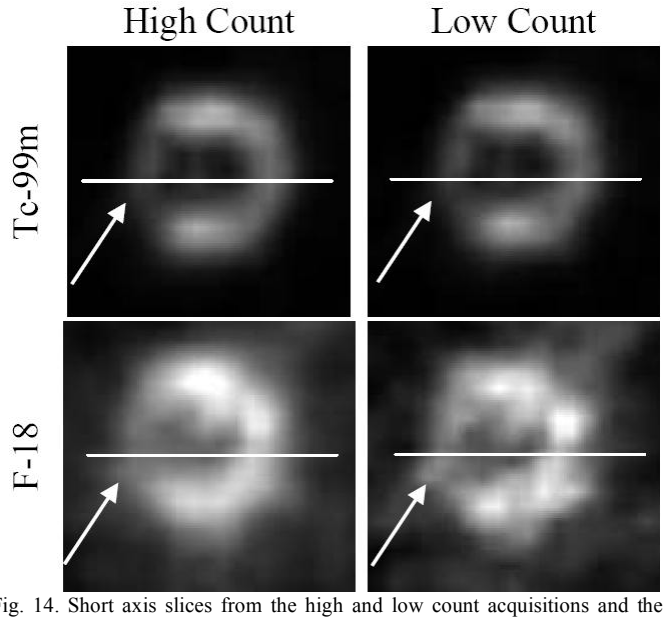

Fig. 14. Short axis slices from the high and low count acquisitions and the location of the profiles. The arrows indicate the location of the defect.

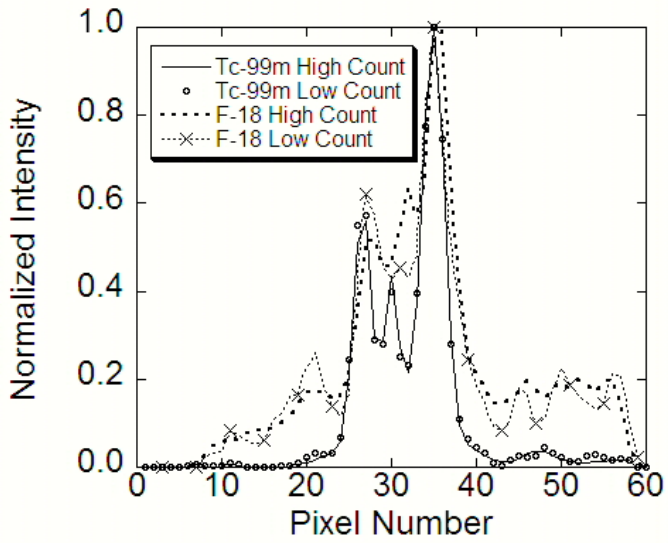

Fig. 15. Normalized line profiles from the high and low count Tc-99m and F-18 acquisitions.

with Tc-99m, the reconstructed image quality did not substantially degrade when the angular sampling was reduced to 19 angles over 180 degrees or to 28 angles over 135 degrees. The results with the F-18 images showed a moderate degree of spatial resolution loss compared with the Tc-99m images. With liver activity present in the F-18 images, a distortion of the myocardial shape was observed, which we attribute to increased detection of septal penetration photons.

Results from the myocardial defect study demonstrate the capability of the mobile SPECT system to image a moderately sized defect, void of activity, with Tc-99m and F-18 distributions. In the Tc-99m images, the defect was readily apparent. In the F-18 images, the quality was degraded by septal penetration of the 511 keV photons in spite of using a high energy collimator. In a clinical setting, it is possible this mobile SPECT system may have difficulty imaging subtle myocardial defects with F-18 tracers, but it may effectively image moderate to severe defects.

The effects of limited angles and septal penetration will depend on the source distribution. We have attempted to mimic realistic source distributions by including extra-myocardial activity in the liver. In patients more areas other than the heart and liver contain activity; therefore, the results from this study may not generalize to all patient studies.

Future work will involve investigating alternate collimators

for the 511 keV SPECT approach, for example, a pinhole collimator [17]-[19]. This type of collimator would more effectively reduce septal penetration effects. Also, the anthropomorphic thorax phantom with the defect will be scanned with the commercial SPECT system. Phantom images acquired on the commercial SPECT system will then be compared to images reconstructed from the mobile system under similar conditions.

REFERENCES

[1] A. G. Weisenberger, S. Majewski, D. Gilland, W. Hammond, B. Kross, J. Proffitt, J. McKisson, and M. Smith. "Implementation of a mobile cardiac PET imager for the emergency room and intensive care unit," *IEEE Nuclear Science Symposium Conference Record*, Vol. 5, 3705-3708, 2007.

[2] M. T. Studenski, D. Gilland, J. Parker, B. Hammond, S. Majewski, A. Weisenberger, and V. Popov. "Performance evaluation of a bedside cardiac SPECT system," *IEEE Trans. Nucl. Sci*. Vol. 56(3), 625-632, 2009.

[3] G. DePuey, E. V. Garcia, D. S. Berman. *Cardiac SPECT Imaging, 2nd Ed*., Lippencott, Williams, and Williams, Philadelphia, PA, 2001.

[4] J. Patton, M. Sandler, I. Ohana, *et al*., "High energy (511 keV) imaging with the scintillation camera," *Radiographics*. 16:1183-1194, 1996.

[5] M. Sandler, J, Bax, J. Patton, *et al*., "Fluorine-18 fluoro-deoxyglucose cardiac imaging using a modified scintillation camera," *J. Nucl. Med*. 39:2035-2043, 1998.

[6] C. Laymon and T. Turkington, "Characterization of septal penetration in 511 keV SPECT," *Nuc. Med. Comm*. 27(11), 901-909, 2006.

[7] E. Q. Chen, W. J. Maclntyre, R. T. Go, R. C. Brunken, G. B. Saha, C. O. Wong, D. R. Neumann, S. A. Cook, and S. P. Khandekar, "Myocardial viability studies using Fluorine-18-FDG SPECT: A comparison with Fluorine-18-FDG PET," *J. Nucl. Med.* 38:582-586, 1997.

[8] M. A. King, R. B. Schwinger, B. C. Penney, P. W. Doherty, and J. A. Bianco. "Digital restoration of Indium-111 and Iodine-123 SPECT images with optimized Metz filters," *J. Nucl. Med.* 27:1327-1336, 1986.

[9] H. H. Barrett and W. Swindell. *Radiological Imaging: The Theory of Image Formation, Detection, and Processing*. San Diego, CA. Academic Press Inc., 1981.

[10] P. F. Sharp, H. G. Gemmell, and A. D. Murray. *Practical Nuclear Medicine, 3rd Ed.*. Springer, New York, NY, 2005.

[11] D. E. Wessell, D. J. Kadrmas, E. C. Frey, and B. M. W. Tsui, "Limited angle tomographic breast imaging: A comparison of parallelbeam and pinhole collimation," *IEEE Nuclear Science Symposium Conference Record*, Vol. 2, pp. 1104-1108, 2-9 Nov 1996.

[12] R. Bartoszynski, M. Niewiadomska-Bugaj. *Probability and Statistical Inference, 2nd Ed.*, Wiley-Interscience, 2008.

[13] S. Cherry, J. Sorenson, and M. Phelps. *Physics in Nuclear Medicine, 3rd Ed*. Philadelphia, PA. Saunders, 2003.

[14] C. E. Metz. "A mathematical investigation of radioisotope scan image processing," Doctoral thesis, University of Pennsylvania, 1969. Ann Arbor, MI. University Microfilms, Publication 70-16-186.

[15] L. A. Shepp, Y. Vardi. "Maximum Likelihood Reconstruction in Positron Emission Tomography," *IEEE Trans. Med. Imag.* 1 (2), 113-122, 1982.

[16] G. Zeng, G. Gullberg, C. Bai, P. Christian, F. Trisjono, E. Di Bella, J. Tanner, H. Morgan, "Iterative reconstruction of Fluorine-18 SPECT using geometric point response correction," *J Nucl. Med*. 39:124-130, 1998.

[17] C. R. Tenney, M. P. Tornai, M. F. Smith, T. G. Turkington, R. J. Jaszczak, "Uranium pinhole collimators for 511-keV photon SPECT imaging of small volumes," IEEE Trans. Nucl. Sci. Vol. 48(4), 1483-1489, 2001.

[18] M. F. Smith, R. J. Jaszczak, and H. Wang, "Pinhole aperture design for I-131 tumor imaging," *IEEE Trans. Nucl. Sci.* Vol. 44:1154-1160, 1997.

[19] M. Smith, R. Jaszczak, H. Wang, and J. Li, "Lead and tungsten pinhole inserts for I-131 SPECT tumor imaging: Experimental measurements and photon transport simulations," *IEEE Trans. Nucl. Sci*. Vol. 44, No. 1, Feb. 1997.

Matthew T. Studenski (M'07) became a member of IEEE in 2007. He was born in Royal Oak, Michigan, in 1983. Matthew received his Bachelor of Science degree in 2005 from the University of Michigan – Ann Arbor in nuclear engineering and radiological sciences. In 2006 he received a Master of Science in Engineering from the University of Michigan – Ann Arbor in nuclear engineering and radiological sciences (health physics). In 2008 he received a second Master of Science degree from the University of Florida in nuclear engineering sciences (medical physics). In 2009 received his PhD from the University of Florida in medical physics with Dr. David Gilland. Matthew's focus is primarily on nuclear medicine and imaging applications. While at the University of Florida, Matthew has published [2].

While finishing his Master of Science in Engineering at the University of Michigan with Dr. Kimberlee Kearfott, Matthew published two articles: 1) M. T. Studenski and K. Kearfott. "Design and Simulation of a Neutron Facility." *Health Physics. Operational Radiation Safety*. 92(2) (Supplement 1): S37-S44, February 2007. and 2) M. T. Studenski, N. Haverland, and K. Kearfott. "Simulation, Design, and Construction of a Cs-137 Irradiation Facility." *Health Physics. Operational Radiation Safety*. 92(5) (Supplement 2): S78-S86, May 2007.

Evaluation of a Bedside SPECT System Based on Cardiac Phantom Defect Detection

Alan T. Cebula[1] , M. T. Studenski[1], A. Samarin[3], D. R. Gilland[1,2]

[1] Dept. of Nuclear and Radiological Engineering, University of Florida, Gainesville, FL, USA

[2] Dept. of Biomedical Engineering, University of Florida, Gainesville, FL, USA

[3] Dept. of Radiology, University of Florida and North Estonia Medical Center, Tallinn, Estonia

OBJECTIVES

- Bedside SPECT imaging of immobile patients and the capability of F-18 imaging in the absence of conventional PET imaging
- Assess the ability of a prototype mobile SPECT system (Fig. 1) to image myocardial defects in an anthropomorphic thorax phantom with either Tc-99m or F-18 activity distributions

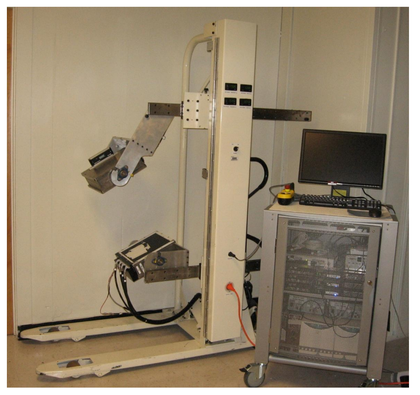

Figure 1. Mobile SPECT system

METHODS AND MATERIALS

- Separately-fillable, cardiac defect (Fig. 2) in myocardium of anthropomorphic thorax phantom (Fig. 3)
- Separate Tc-99m and F-18 studies (Table1)
- Defect contrast (Eqn. 1)

$$CONTRAST = \frac{MYOCARDIUM - DEFECT}{MYOCARDIUM} x\ 100\% \qquad (1)$$

- 25 projection angles over 180 degrees, out-of-field liver activity, with high count acquisition times of 45 (Tc-99m) and 60 (F-18) minutes
- Binomial thinning to simulate low count acquisition times of 15 (Tc-99m) and 20 (F-18) minutes with 200 µCi total activity in myocardium and 400 µCi total activity in liver
- Metz filter based on measured MTF (Eqn. 2, Fig. 4)

$$P(s_x, s_y) = \frac{1 - (1 - MTF(s_x, s_y)^2)^N}{MTF(s_x, s_y)} \qquad (2)$$

- Pre-filtered projection data reconstructed using 50 iterations of an MLEM algorithm
- Short axis reorientation and profiles through myocardial defect region

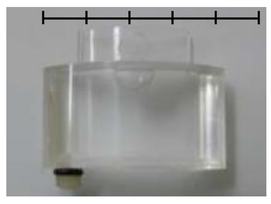

Figure 2. Photograph of the cardiac defect (scale: cm)

Table 1. Parallel Hole Collimator Parameters [mm]

Activity	Flat-Flat Distance	Septa Thickness	Hole Length
Tc-99m	1.5	0.20	23
F-18	2.3	2.02	49

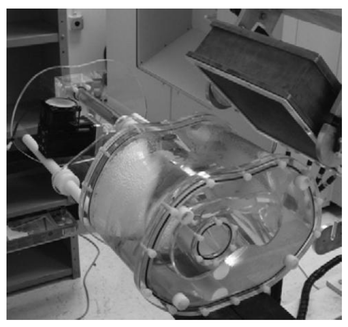

Figure 3. Anthropomorphic thorax phantom [2]

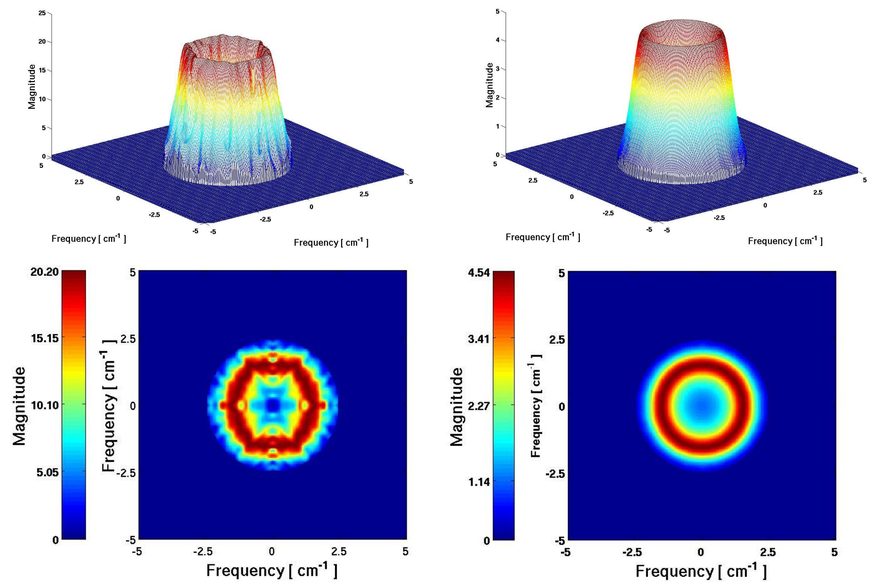

Figure 4. Left: Anisotropic F-18 Metz filter (N=1000) due to anisotropic septal penetration Right: Tc-99m Metz filter (N=50) [1]

RESULTS

- Effect of septal penetration from out-of-field activity and Metz filter on projection data (Fig. 5)
- Three slices of short axis images through defect region for each acquisition (Figs. 6,7)
- Contrast of defect shown in line profiles (Fig. 8)

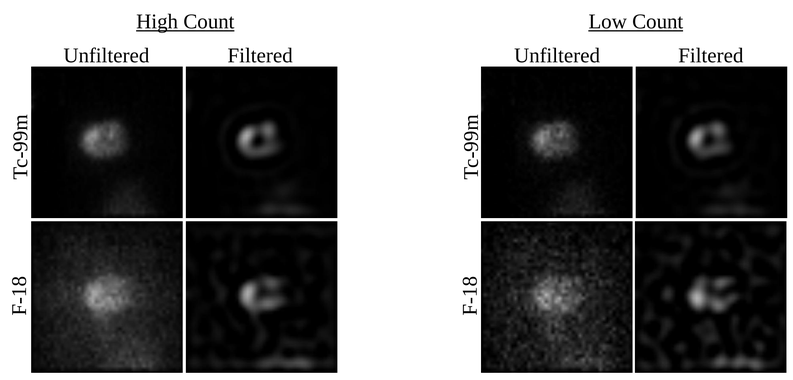

Figure 5. Unfiltered and Filtered projection data for 100% contrast defect

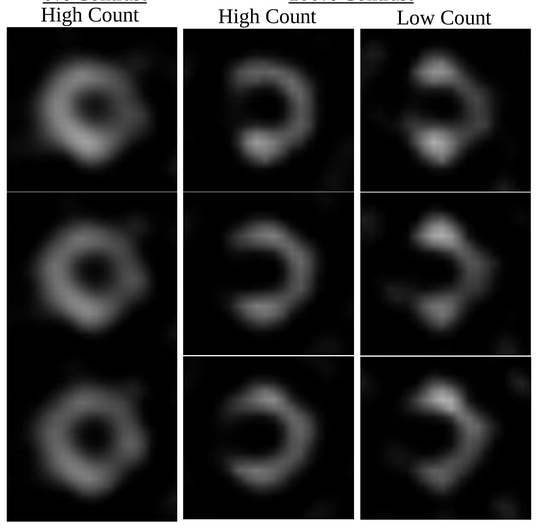

Figure 6. F-18 short axis images

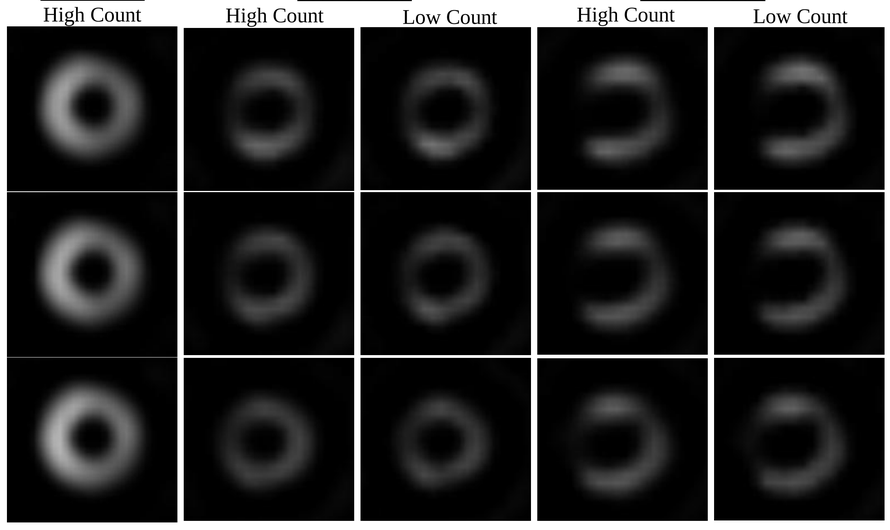

Figure 7. Tc-99m Short axis images

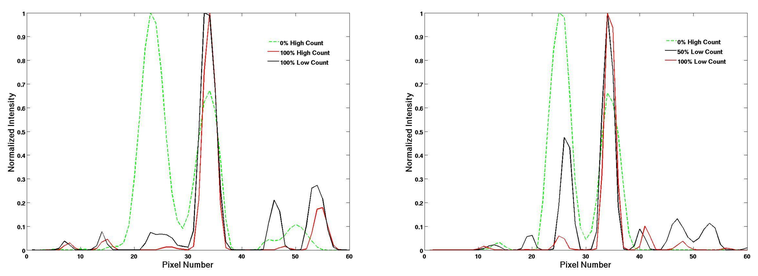

Figure 8. Line profiles through defect region for F-18 (left) and Tc-99m (right)

CONCLUSIONS AND FUTURE WORK

- Results demonstrate the capability of the system to image a myocardial defect in a thorax phantom for both Tc-99m and F-18 activity distributions with acquisition time of 15 (Tc-99m) and 20 (F-18) minutes
- Metz filter mitigates the effect of septal penetration photons
- Capable of F-18 SPECT imaging in the absence of conventional PET imaging
- Future work includes determining the effects of reduced angular sampling, characterizing the system for pinhole SPECT, and performing an ROC study

UF UNIVERSITY of FLORIDA GATOR Engineering

References

1. M.T. Studenski, D. Gilland, J. Parker, B. Hammond, A. Weisenberger, and V. Papov, “Performance evaluation of a bedside cardiac SPECT system," *IEEE Trans. Nucl. Sci.* vol. 56, 2009, in press.
2. Model ECT/DY-CAR/P, Data Spectrum Corp. Hillsborough, NC, 27278

Support provided by the United States Army Medical Research and Material Command under Award No. W81XWH-04-1-0594

Poster display number: M13-54